Electronic Supplementary Material (ESI) for Soft Matter.

Vesicle deformation and division induced by flip-flop of lipid molecules

Naohito Urakami[a], Yuka Sakuma[b], Toshikaze Chiba[b], and Masayuki Imai[b]

[a.] Department of Physics and Informatics, Yamaguchi University, 1677-1 Yoshida, Yamaguchi, 753-8512, Japan. E-mail: urakami@yamaguchi-u.ac.jp

[b.] Department of Physics, Tohoku University, Aoba, Sendai 980-8578, Japan.

1. Equilibrium spherical vesicle.

We obtained the equilibrium spherical vesicle as the following procedure: We first prepared a spherical single-component vesicle composed of 6,500 ZLs and a spherical binary vesicle composed of 52,00 ZLs and 13,00 NLs. Notably, the initial spherical vesicles have slight large number of water beads inside them. During the simulation, the transfer of water beads between the inside and outside of the vesicle and flip-flops between the inner and outer leaflets occurs. Thus, after the number of water beads inside vesicle (N_w) and the difference in the number of lipids between the outer and inner leaflets (ΔN) were relaxed enough, we obtained vesicles as the equilibrium spherical vesicle.

As shown in Fig. S1, after the simulation started, N_w initially decreases. The decreases in N_w for the single-component vesicle and binary vesicle stopped at 400,000τ and 200,000τ, respectively. We carried out more 200,000τ simulations to obtain the equilibrium spherical vesicle. For ΔN, no significant change was observed for both of single-component and binary vesicles as shown in Fig. S2. Here, comparing with the single-component vesicle, the fluctuation of ΔN for the binary vesicle is very fast. This is because the flip-flop rate of NLs is much faster than that of ZLs. From these results, we treated vesicles after 400,000τ for the single-component vesicle and after 200,000τ for the binary vesicle as the equilibrium spherical vesicles.

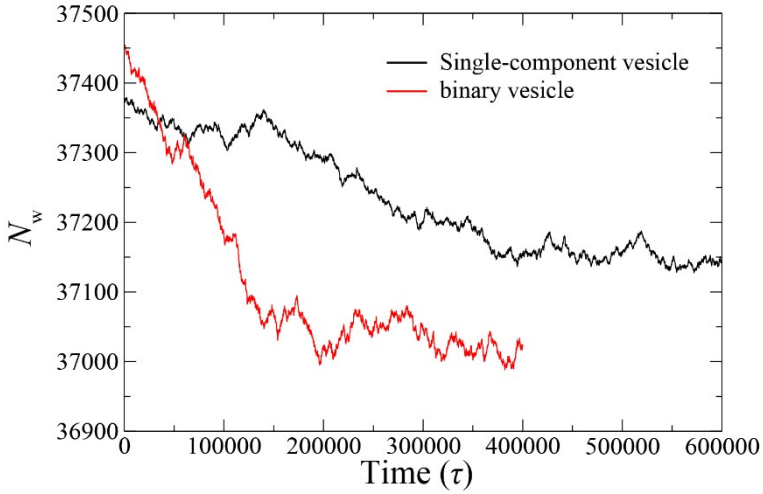

Fig. S1. Time evolution of the number of the water beads (N_w) for the single vesicle (black line) and the binary vesicle (red line).

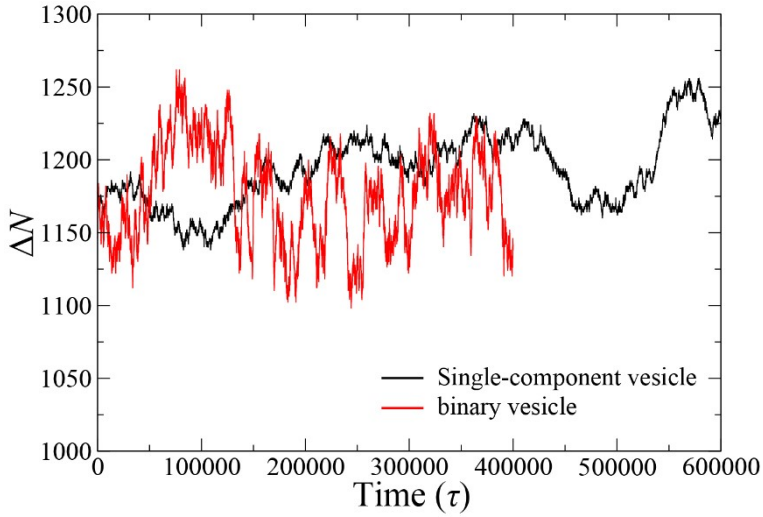

Fig. S2. Time evolution of the preferred area difference (ΔN) for the single vesicle (black line) and the binary vesicle (red line).

2. Vesicle deformation from the initial vesicle having $\Delta\phi_0 = -0.5$.

In our simulations, binary SUVs composed of ZLs and NLs showed vesicle division for $\Delta\phi_0 \leq -0.37$. To attain the vesicle division, the SUVs should deform to the limiting shape, however, the binary SUVs with $\Delta\phi_0 > -0.37$ failed to deform to the limiting shape as shown in Figs. 5 and 6(a) in the main text. Thus, the key to attain the vesicle division is the deformation to the limiting shape. There are two explanations for the observed vesicle division. One is the flip-flop induced vesicle division as described in the main text, where the flip-flop of NLs in the inner leaflet to the outer leaflet increases Δa_0, resulting in deformation to the limiting shape. Another one is that the stable state of the initial binary SUV with the effective spontaneous curvature, $c_0 = H_{sp}^{NL}\Delta\phi_0$, is the limiting shape. Examined binary SUVs in section 3.4 have initial normalized preferred area difference of Δa_0^{asy} =1.61 [Fig. 6(a)] and the spontaneous curvature modifies the preferred area difference as $\Delta a_0^{sym} = \Delta a_0^{asy} + R_s c_0/2q$, where Δa_0^{sym} is the normalized preferred area difference for symmetric bilayer (no spontaneous curvature, *i.e.* $\Delta\phi_{NL} = 0.0$). When the value of Δa_0^{sym} is greater than ~1.80, then the SUVs will deform to the limiting shape. Here we calculate Δa_0^{sym} of the binary SUV with $\Delta\phi_0 = -0.5$. The SUV has $c_0 = H_{sp}^{NL}\Delta\phi_0 = 0.075$ nm^{-1} ($H_{sp} \approx -(1 - R_{h/t})/d = -0.15$ nm^{-1}), $R_s = 11.8$ nm, and we assume $q = 3$, then we obtain $\Delta a_0^{sym} = 1.75 \approx 1.80$, which indicates that this vesicle might deform to the limiting shape. Then, we carried out a CGMD simulation for the binary SUV ($\Delta a_0 = 1.61$ and $\Delta\phi_0 = -0.5$) to examine effects of the flip-flop motion on the vesicle deformation. To prevent the flip-flop motion, we increased the repulsive interaction between the hydrophilic bead and hydrophobic bead. Thus, we modified σ_{HT} between head beads and tail beads of ZLs and NLs as $\sigma_{H(ZL)T(ZL)} = 1.0 \rightarrow 1.5$, $\sigma_{H(ZL)T(NL)} = 1.1 \rightarrow 1.5$, $\sigma_{H(NL)T(ZL)} = 0.9 \rightarrow 1.5$, $\sigma_{H(NL)T(NL)} = 1.0 \rightarrow 1.5$. The modification is only applied to the interaction between head beads (#1) and tail beads (#5 and #6) of ZLs and NLs in Fig. S3, which will minimize the influence of the modification on the membrane. Fig. S4 shows the time evolution of the numbers of ZLs (N_{ZL}^-) and NLs (N_{NL}^-) in the inner leaflet of vesicle. For $\sigma_{HT} = 1.5$, N_{ZL}^- and N_{NL}^- remained at their initial values during $15{,}000\tau$ simulation run, indicating that the flip-flop is suppressed. On the other hand, when we used the original potential, we observed an increase in N_{ZL}^- and a decrease in N_{NL}^- (Fig. S4). If we suppress the flip-flop motion ($\sigma_{HT} = 1.5$), no significant deformation from the initial vesicle shape (no vesicle division) was observed during $15{,}000\tau$ simulation run [Fig. S5(a)], while if we use the original potential (with flip-flop motion), the vesicle division was observed at $11{,}500\tau$ [Fig. S5(b)]. These simulations indicate that the vesicle division is induced by the flip-flop motion.

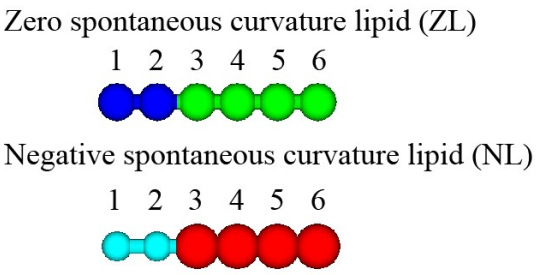

Fig. S3. Coarse-grained model for lipid molecules. (Top) Zero spontaneous curvature lipid (ZL). (Bottom) Negative spontaneous curvature lipid (NL). Hydrophilic head beads are depicted in blue and cyan, and hydrophobic tail beads are depicted in green and red for ZL and NL, respectively. The numbers above the beads represent the bead number. We just changed to $\sigma_{HT} = 1.5$ between the head bead (#1) and the tail beads (#5 and #6) for both of ZLs and NLs to minimize the influence of the potential change on the membrane.

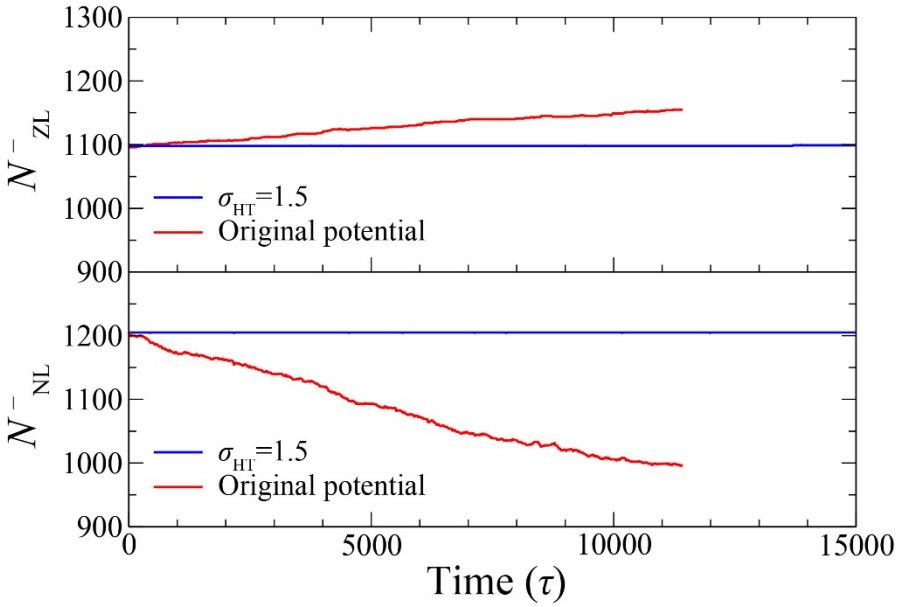

Fig. S4. Time evolution of $N_{\bar{ZL}}$ (upper plot) and $N_{\bar{NL}}$(lower plot). Blue and read lines represent the time evolution for large $\sigma_{HT} = 1.5$ and for the original potential. We carried out the simulation from the same initial vesicle at $\Delta a_0 = 1.61$ and $\Delta\phi_0 = -0.5$.

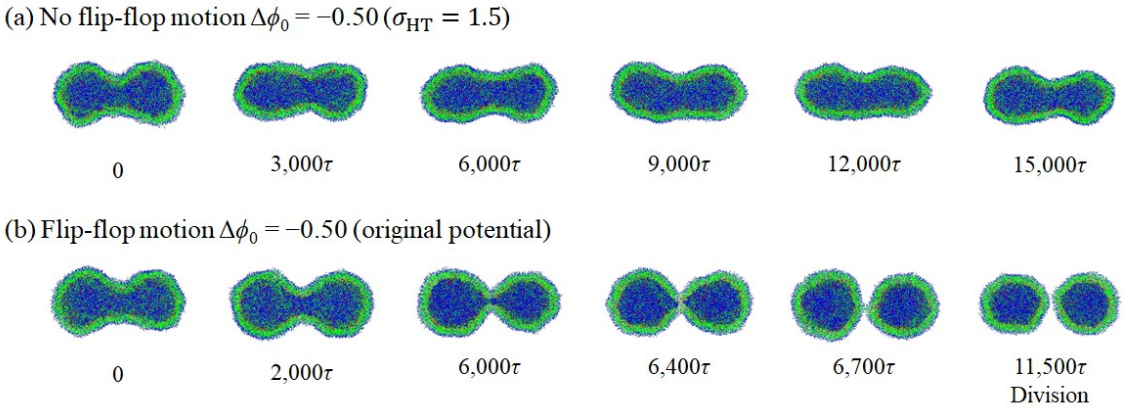

Fig. S5. Time evolution of vesicle deformation from the initial vesicle at $\Delta a_0 = 1.61$ and $\Delta\phi_0 = -0.5$ for $\sigma_{HT} = 1.5$ (a) and for the original potential (b). The water beads inside the vesicle are depicted in blue.

3. Vesicle deformation and division of vesicle having $\Delta a_0^{asy} = 1.35$ and $\Delta\phi_0 = -0.5$ as an initial state.

Furthermore, to examine the effect of the spontaneous curvature on the vesicle division, we carried out a simulation for the binary SUV having initial $\Delta a_0^{asy} = 1.35$ and $\Delta\phi_0 = -0.5$. In this case, the initial SUV has $\Delta a_0^{sym} = 1.35 + 0.14 = 1.49$, which is much lower than the limiting shape $\Delta a_0^{sym} = 1.8$. Fig. S6 (a) shows the time evolution of Δa_0^{asy}, and snapshots of vesicles during the deformation process. With elapse of time, Δa_0^{asy} increased monotonically and the SUV deformed from prolate to the limiting shape, and finally, the vesicle division was observed at $\sim 15{,}000\tau$. In this simulation, N_{ZL}^{-} increased from 1,200 to 1,250, while N_{NL}^{-} decreased from 1,250 to 950, which indicates that the flip-flop of NLs increased Δa_0 [Fig. 6(a)] and $\Delta\phi_{NL}$ [Fig. S6(c)]. The observed time evolution of Δa_0, N_{ZL}^{-}, N_{NL}^{-}, and $\Delta\phi_{NL}$ agreed with those of the SUVs with $\Delta a_0^{asy} = 1.61$ and $\Delta\phi_0 \leq -0.37$ (Fig. 6 in the main text). Therefore, we conclude that the vesicle division is induced by the flip-flop of NLs, not by the initial spontaneous curvature.

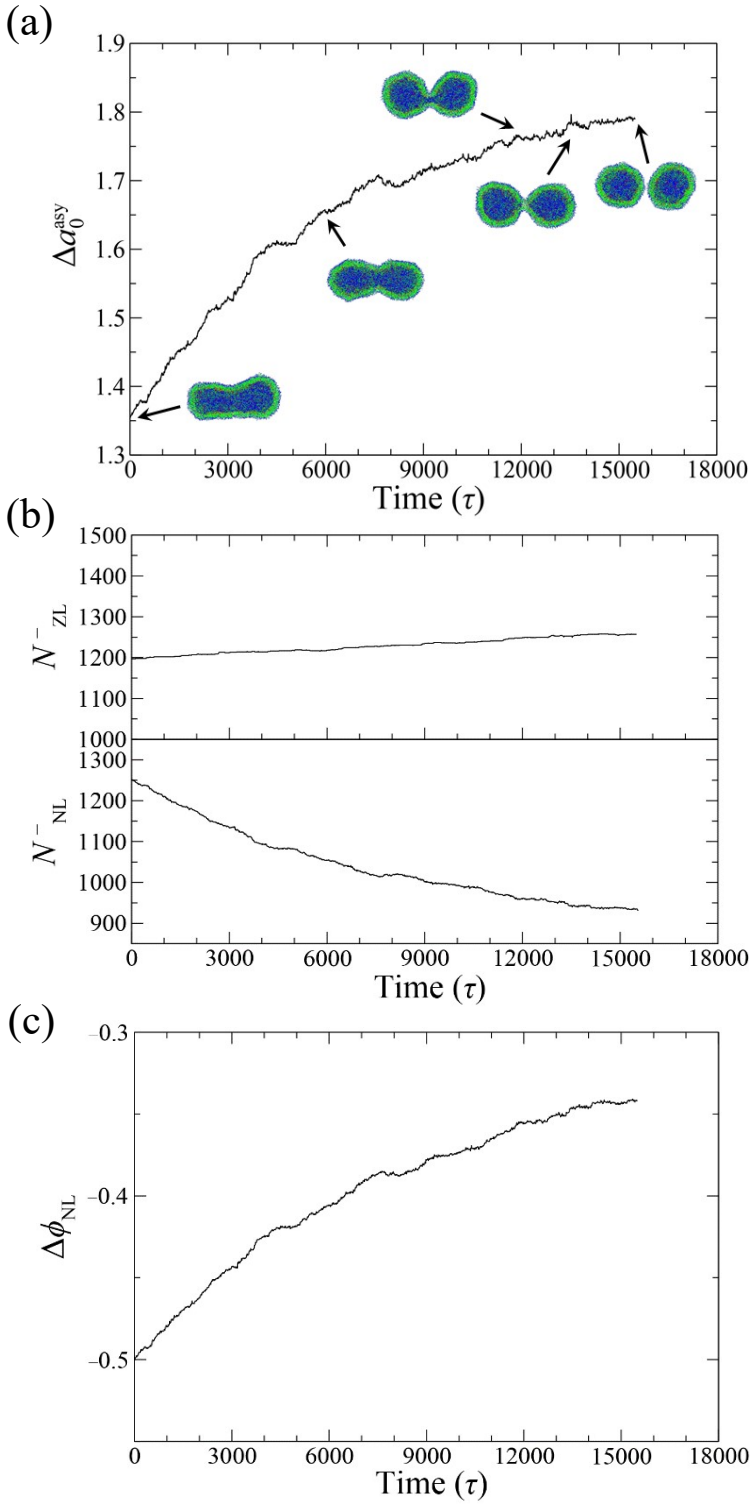

Fig. S6. Time evolution of (a) Δa_0^{asm}, (b) N_{ZL}^{-} (upper plot), N_{NL}^{-}(lower plot), and (c) $\Delta\phi_{NL}$ for the initial vesicle shape having $\Delta a_0^{asm} = 1.35$ and $\Delta\phi_0 = -0.5$. Snapshots in panel (a) represent the typical vesicle shapes obtained in the simulations. The water beads inside the vesicle are depicted in blue.